The Journal of Neuroscience, July 1987, 7(7): 2214–2231

Regional Distribution of Astrocytes with Intense Immunoreactivity for Glutamate Dehydrogenase in Rat Brain: Implications for Neuron–Glia Interactions in Glutamate Transmission

Chiye Aoki, Teresa A. Milner, Kwan-Fu Rex Sheu,[1] John P. Blass,[1] and Virginia M. Pickel

Department of Neurology, Cornell University Medical College, New York, New York 10021, and [1]Dementia Research Service, Burke Rehabilitation Center, White Plains, New York 10605

The principally mitochondrial enzyme glutamate dehydrogenase (GDH) exhibited low-intensity, uniform immunoreactivity in neurons and intense heterogeneous labeling of glial cells of rat brain. Simultaneous peroxidase labeling for GDH and immunoautoradiography for glial fibrillary acidic protein (GFAP) confirmed the astrocytic localization of the enzyme. Immunoreactivity in astrocytes, but not in neurons, required the presence of Triton X-100 as a solubilizing agent. Most of the intensely labeled glial processes were localized to regions previously reported as containing moderate to high densities of binding sites for the excitatory amino acids, L-glutamate or L-aspartate, and glutamatergic fibers. These included several forebrain regions, such as the superficial layers of the rostral neocortex, dorsal neostriatum, nucleus accumbens, septohippocampal nucleus, intralaminar thalamic nuclei, and external capsules. However, the central gray of the midbrain, the nuclei of the reticular formation, brain stem regions projecting to the cerebellum, and cranial nuclei of the trigeminal and vagal nerves also exhibited intense glial labeling for GDH, even though some of these regions are known to receive only weak glutamatergic projections. A second factor determining the distribution of GDH appeared to be neuronal activity, as assessed by correspondence with reported high densities of cytochrome oxidase. We conclude that GDH enriched in glial populations (1) exists in a subcellular compartment distinct from that of neurons and (2) may serve as one of the enzymes involved in glutamatergic transmission. Deficiencies of glial GDH and the consequent cytotoxic effects of high levels of excitatory amino acids may contribute to a number of neurodegenerative disorders.

Received Aug. 29, 1986; revised Dec. 30, 1986; accepted Jan. 22, 1987.

This study was supported by NIH Grants 5F32NS07782 (C.A.), HL18974, and MH40342 (V.M.P.); by NS22952 (K.-F.R.S.), AG03573 (J.P.B.), and the Will Rogers Institute (J.P.B.). V.M.P. is also supported by a career award from the NIMH (MH00078) and NSF Grant BNS 80-23914. We wish to thank Drs. David Ruggiero, Joseph LeDoux, and Victoria Arango for their anatomical expertise; Dr. Young-Tai Kim for providing Sepharose-conjugated antibodies; June Chan and Dr. Harriet Baker for their technical assistance; and Nancy Marmor, Hillary Rettig, and William Feig for their assistance with the preparation of the manuscript.

Correspondence should be addressed to Chiye Aoki, Department of Neurology/Neurobiology, Cornell University Medical College, 411 E. 69th Street, New York, NY 10021.

Glutamate dehydrogenase (GDH; L-glutamate : NAD oxidoreductase; E.C.1.4.1.2) is one of the major enzymes involved in the interconversion of glutamate and alpha-ketoglutarate of the tricarboxylic acid cycle (Dennis and Clark, 1977). Thus, GDH might be expected to be present in mitochondria of both glia and neurons throughout the brain. However, since glutamate is also an excitatory transmitter in selective neuronal pathways (Cotman et al., 1981; Watkins and Evans, 1981; Fonnum, 1984), higher concentrations of the enzyme also might be expected in corresponding neurons or their associated glia. The glial versus neuronal, or the dual glial and neuronal localization of GDH in brain has been contested for a number of years (see Nicklas, 1984, for a review). Furthermore, the regional concentrations of GDH relative to glutamatergic pathways have not been extensively examined by cytochemical methods (Graham and Aprison, 1969; Ryder, 1980; Wenthold, 1980; Leong and Clark, 1984).

In the present study we employed the peroxidase–antiperoxidase (PAP) immunocytochemical method (Sternberger, 1979) for determining the cellular and regional distributions of GDH in adult rat brain. The glial versus neuronal labeling was distinguished by the dual localization of GDH and of glial fibrillary acidic protein (GFAP) (Bignami et al., 1972) using combined PAP and immunoautoradiographic methods (Pickel et al., 1986). Furthermore, since GDH is believed to exist in at least 2 forms, differing in susceptibilities to solubilization by detergents and salts (Colon et al., 1986; Lai et al., 1986), we examined the immunocytochemical localization of the enzyme under a variety of fixation conditions, using different concentrations of detergents in the labeling procedure.

Materials and Methods

Antisera. The antiserum to GDH was prepared by immunizing rabbits with bovine liver GDH (Sigma) that had been further purified by SDS–PAGE. This antiserum has been tested for its specificity by the detection of a single immunoreactive material on immunoblots, using GDH purified from bovine liver, as well as GDH in whole homogenates of brain (Lai et al., 1986).

Rabbit PAP and rabbit anti-GFAP antiserum were generously supplied by the laboratories of Dr. T. H. Joh (Cornell University Medical College, New York) and Drs. A. Bignami and D. Dahl (V. A. Medical Center, MA), respectively. Donkey anti-rabbit ^{125}I-IgG was obtained from Amersham, and goat anti-rabbit IgG from Miles Laboratory (Elkhart, IN).

Fixation and sectioning. Thirty-two adult (180–250 gm) male rats were perfused for 6 min through the ascending aorta with one of 3 fixatives. These were (1) 200 ml of 4% paraformaldehyde in 0.1 M phosphate buffer (pH 7.4); (2) 50 ml of 3.75% acrolein and 2% paraformaldehyde, followed by 150 ml of 2% paraformaldehyde; and (3)

4% paraformaldehyde with 0.1–0.2% glutaraldehyde. After the termination of perfusion, the brains were removed, cut into 1 mm coronal or sagittal blocks and further fixed in 2 or 4% paraformaldehyde for ½ hr. With each of the 3 fixation conditions, the 1 mm blocks were sectioned at 30–50 μm on a Vibratome or were cryoprotected with 10% sucrose in 0.1 M phosphate buffer, rapidly frozen in freon, then sectioned on a sliding microtome. Both types of sections were collected in 0.1 M Tris–0.9% NaCl buffer (Tris-saline) at pH 7.6.

Single-labeling with the GDH and the GFAP antisera. The fixed sections were immunocytochemically labeled by a modification (Pickel, 1981) of the PAP method of Sternberger (1979). Prior to the incubation of sections with the antiserum, they were incubated for ½ hr with 3% goat serum–Tris-saline. This buffer, with the substitution of 3% goat serum with 1% goat serum, was used in all of the subsequent incubations and in the rinses between incubations. Sections were incubated with GDH or GFAP antiserum for a period of 12–48 hr and at dilutions from 1:800 to 1:5000. Sections were then incubated in the goat anti-rabbit IgG at a dilution of 1:50 for 1 hr, followed by an incubation in the rabbit PAP at a dilution of 1:100 for 1 hr. Following 2 rinses in Tris-saline not containing goat serum, the peroxidase was demonstrated by reaction with 3′,3′-diaminobenzidine and H_2O_2.

For the purpose of enhancing the penetration of the antisera, some sections were permeabilized with 0.25% (vol/vol) Triton X-100 or (wt/vol) saponin. In these cases, the detergent was added to all incubation and wash solutions. All incubations and washes were carried out at room temperature.

Preadsorption of the GDH-antiserum with GDH. Bovine liver GDH was coupled to cyanogen bromide-activated Sepharose 4B beads (Pharmacia), according to the manufacturer's instructions. Two milliliters of anti-GDH antiserum (ca. 40 μg of IgG, 40 mg of total protein) were incubated with 100 μl of GDH coupled to Sepharose beads (100 μg of GDH) for 1 hr at 37°C under gentle agitation. The supernatant formed by a 1 min centrifugation at 100 × *g* was collected and substituted for the specific antiserum in the labeling procedure.

Dual labeling for GDH and GFAP. The antisera to GDH and GFAP were raised in rabbits. Thus, one antiserum had to be localized using a dilution sufficiently high to be recognized by autoradiography of ^{125}I-labeled secondary antibody, but not by the peroxidase method, as was described recently in detail (Pickel et al., 1986). The sections were first incubated with the GFAP antiserum at a dilution of 1:30,000, which was determined to be the highest possible dilution that allowed for reasonable detections of the immunoreactivity by autoradiography, but not by peroxidase. Following a 12–16 hr period of incubation with or without 0.25% Triton X-100, sections were incubated in a buffer containing a 1:50 dilution of donkey anti-rabbit ^{125}I-IgG (100 μCi/ml) for 2 hr. This step was followed by 10 rinses over a period of 5 hr to remove unbound ^{125}I-IgG. The tissue was then incubated with the GDH antiserum at a dilution of 1:2000 for 48 hr in the presence of 0.2% Triton X-100. All dilutions and washes were in Tris-saline (pH 7.6) containing 1% goat serum, and the entire labeling procedure was carried out at room temperature, with continuous agitation. The immunoreactivity for GDH was detected by the accumulation of peroxidase products, and the immunoreactivity for GFAP was detected autoradiographically. For the purpose of autoradiography, after the PAP reaction sections were mounted on slides, dehydrated, then rehydrated through ethanol and dipped in Ilford L4 emulsion (at 50°C) diluted 1:1 with distilled water. These slides were air-dried, then stored with a desiccant in light-tight boxes at 4°C for 4–24 d exposure periods. The autoradiographs were developed at the end of the exposure period and examined with a Nikon Microphot FX using either bright-field or differential-interference contrast optics. The extent of labeling of the rabbit GFAP antiserum by the rabbit PAP was monitored by examining sections that were processed as described above in the absence of the GDH antiserum.

Other cytochemical and histochemical methods. Sections adjacent to the ones used for immunocytochemistry were processed for cytochemical and histochemical procedures to facilitate neuroanatomical identification of the immunoreactive structures. The histochemical procedure for the demonstration of AChE has been described previously by Hedreen et al. (1985).

Presentation of labeling with the GDH antiserum. The immunoreactive structures were mapped using a camera lucida attachment on a Leitz microscope. The boundaries of nuclei and fiber tracts, which were difficult to distinguish on the immunocytochemically stained sections, were delineated using both adjacent Nissl and AChE-stained sections. Nomenclature for the nuclei and fiber tracts was from the atlas of Paxinos and Watson (1982). In addition, identifications of some of the thalamic nuclei and neocortical regions were modified in accordance with the delineation of boundaries of Jones (1985) and Peters and Jones (1984). Each stippling on the schematics of Fig. 6, *A–J,* represents 10–15 processes. When the processes appeared to be regularly oriented within structures, stippled lines were drawn to reflect the direction of the labeled profiles.

Results

Under a specific set of experimental labeling conditions, GDH was selectively localized to glial cells. These GDH-enriched glial cells were heterogeneously distributed in rat brain. The experimental labeling conditions, morphological and chemical characteristics of identified glial cells, and distribution of the labeled cells are described in the following sections.

Labeling conditions

Vibratome sections of brains fixed with paraformaldehyde alone or combined with low (0.1–0.2%) concentrations of glutaraldehyde showed immunocytochemical labeling with GDH antiserum. Intense immunoreactivity was seen in glial cells when 0.2% Triton X-100 was included in all incubations (Fig. 1, *A, C, E*) (see next section for identity of cell types). Changes in the fixation condition, sectioning procedure, and use of lipid solvents markedly altered the intensity of the glial labeling for GDH. For example, omission of glutaraldehyde increased, whereas addition of acrolein decreased, the intensity of labeling in Vibratome sections with the use of Triton X-100 in all incubations. In brains fixed with 4% paraformaldehyde, frozen and sectioned on a sliding microtome, and immunostained in the presence of Triton X-100, the peroxidase product in glia was greatly reduced. The substitution of saponin for Triton X-100 in the immunocytochemical labeling of paraformaldehyde-fixed Vibratome sections also produced less intense labeling in glia. *In the absence of Triton X-100,* similarly prepared sections showed only a diffuse background labeling and a low intensity of immunoreactivity in larger cells, presumed to be neuronal perikarya, in the striatum and in most other regions (Fig. 1, *B, F*). However, in areas such as the neocortex, the labeling in the cytoplasm of neuronal perikarya was more intense and punctate, particularly with higher concentrations (0.2%) of glutaraldehyde (Fig. 1*D*). Both glial and neuronal labeling were abolished when the primary antiserum was adsorbed with purified GDH prior to the immunocytochemical labeling (Fig. 1, *G, H*) and thus represented specific labeling for the enzyme.

Identification of glial cells

In Vibratome sections of paraformaldehyde-fixed tissues immunolabeled for GDH *in the presence of Triton X-100,* intense peroxidase reaction product was detected in round or spindle-shaped cells having a thin rim of cytoplasm, multiple long (10–50 μm) branched processes, and small round or angular nuclei (Fig. 1, *A, C, E*). These cytological features, combined with their location in cellular portions of the neuropil and in fiber bundles, led to a tentative identification of protoplasmic and fibrous astrocytes (Figs. 1–6; described below in detail). Other presumed glial processes containing immunoreactivity for GDH were seen exclusively in areas, such as layer I of the anterior cingulate cortex (ACg; Fig. 2, *A, C*). These straight, twiglike processes were 10–20 μm in length, and clustered in tight bundles containing 3–5 processes.

The GDH-labeled processes along blood vessels were in a

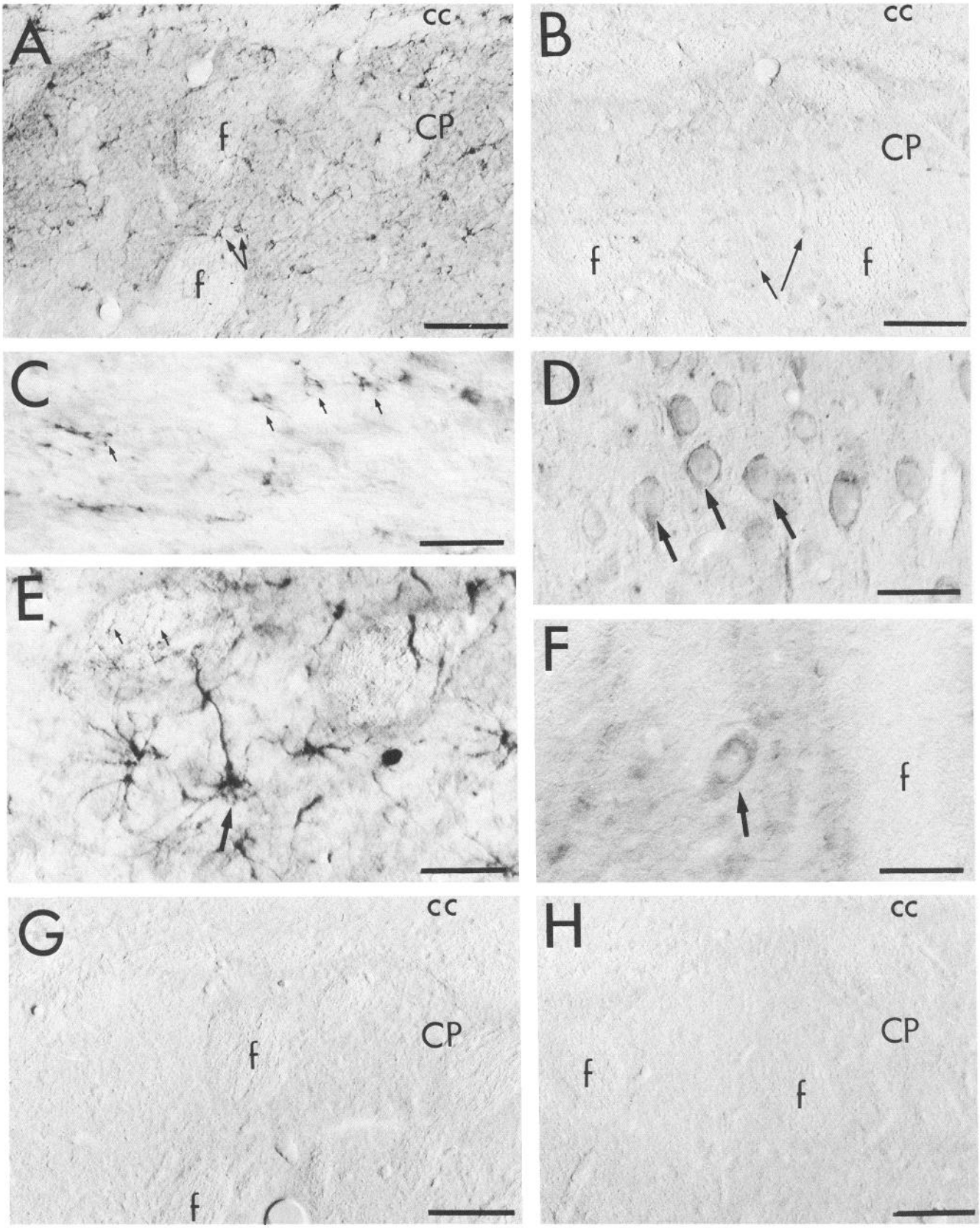

Figure 1. Cellular localization of GDH in relation to methods of tissue preparation. *A–C, E, G, H,* Fixation with 4% paraformaldehyde and 0.1% glutaraldehyde. *D, F,* Fixation with 4% paraformaldehyde and 0.2% glutaraldehyde. Micrographs in *G* and *H* show sections through the caudate putamen (*CP*) immunolabeled with control serum in the presence (*G*) and absence (*H*) of Triton X-100. Micrographs in *A* and *B* show sections through the CP immunolabeled with GDH antiserum in the presence and absence of Triton. *C, E,* Higher magnifications of the GDH labeling in the corpus callosum (*CC*) and CP of sections prepared as in *A*. *Arrows* in *A, C,* and *E* show glial labeling. *D, F,* Higher-magnification micrographs

similar pattern to the GFAP-immunoreactive processes, as seen at low (Fig. 2, *A, B*) and high (Fig. 2, *C, D*) magnifications of the ACg. However, the GDH-labeled cells and processes were far less numerous than those labeled with the GFAP antiserum in most areas examined. For example, in the ACg (Fig. 2*B*) and in the hippocampus, GFAP-immunoreactive cells were prominent throughout all layers. In contrast, labeling with the GDH antiserum was enriched in the superficial layers in the ACg (Figs. 2*A* and 6, *B–D*) and within the stratum lacunosum-moleculare of the hippocampus (Fig. 6, *E, F*, just dorsal to the hippocampal fissure), particularly in association with the walls of major blood vessels. In other examples, the GFAP-labeled processes showed little structural resemblance to the straight, twiglike processes containing immunoreactivity for GDH (Fig. 2, *C* vs *E*).

The labeling pattern in the cerebellum was more dramatically divergent. The radiating processes of glia, especially within the outer molecular layer, but also within the granule cell layer, were prominently labeled with the GFAP antiserum (Fig. 3*B*). In contrast, labeling for GDH was more moderate and within the finer-caliber fibers of the molecular layer and diffuse within the granule cell layer (Fig. 3*A*).

The dorsal medulla oblongata was one of the regions that exhibited a close correspondence between the patterns of labeling for GDH and GFAP. With both antisera, the labeling was intense within the nucleus of the solitary tract (NTS) and dropped sharply at the boundary to the motor nucleus of vagus (X) (Fig. 4, *A, B*).

In dual-labeling studies with dilutions sufficient to differentiate the 2 rabbit antisera, GDH was shown to be colocalized with GFAP in subsets of cells located in the neuropil and in fiber bundles (Fig. 5). The dual labeling was detected in both the radiating, branched processes (double arrows in Figs. 5, *A, B, D, F*) and in straight, twiglike processes (single arrow in Fig. 5*A*). In most cases, the silver grains that developed from the ^{125}I-IgG bound to the GFAP antiserum were concentrated over only a portion of the peroxidase-labeled GDH cells or processes. In every region examined, cells exhibiting only silver grains (GFAP), only peroxidase (GDH immunoreactivity; arrowheads in Fig. 5, *A, D*) and both of the labels were found.

Distribution of GDH-labeled cells and processes

Forebrain

In the forebrain, dense as well as sparse labeling for GDH was seen in different subregions of the (1) neocortex, (2) hippocampus, (3) basal ganglia, (4) other telencephalic subnuclei, (5) thalamus, (6) hypothalamus, as well as in (7) fiber tracts.

Neocortex. Immunolabeling within layer I and along orthogonally oriented large blood vessels decreased in the rostrocaudal direction. Specifically, the most prominent labeling was seen in the ACg (Fig. 6, *B–D*), the primary olfactory cortex (PO), and tubercle (Tu) (Fig. 6, *A–E*). Less labeling was found in the posterior cingulate (PCg; Fig. 6*E*) and entorhinal (Ent; Fig. 6*F*) cortices and the subiculum (S; Fig. 6*F*). These processes were morphologically distinct from the radiating processes that extended outward from the corpus callosum (cc) in layer VI (Fig. 6, *A, B*).

Hippocampus. Twiglike processes containing GDH immunoreactivity were densely distributed throughout the anterior–posterior extension of the stratum lacunosum-moleculare of the hippocampus (Fig. 6, *E, F*, just dorsal to the hippocampal fissure). These processes were in close association with blood vessels that coursed parallel to the hippocampal fissure. A few more delicately branched processes with GDH immunoreactivity were seen throughout all layers of the hippocampus and the dentate gyrus (DG), and running in parallel with the axons in the alveus. Diffuse labeling for GDH was most evident in the stratum lacunosum-moleculare of CA1 and CA3, but was also detectable in the pyramidal cell layer of CA1.

Basal ganglia and associated nuclei. In the neostriatum (caudate-putamen complex), GDH was localized to numerous cells with long, wispy processes (Figs. 1, *A, E*; 5*D*; 6, *B–E*) that were frequently associated with blood vessels coursing in an anterior–posterior direction. Occasionally, labeled twiglike processes could also be identified within the dorsolateral quadrant.

The medial–ventral quadrant of the striatal complex, corresponding to the accumbens nucleus (Acb; Fig. 6, *A, B*), the ventral pallidum (VP; Fig. 6, *B–D*) and nucleus basalis (B; Fig. 6*D*), and the more lateral endopyriform nucleus (En; Fig. 6, *B–E*) and claustrum (Cl; Fig. 6, *A–D*), were particularly rich in processes with GDH immunoreactivity. In contrast, the substantia innominata (SI; Fig. 6*D*) and the nucleus of the anterior commissure (AC; Fig. 6, *C, D*) were only moderately labeled. The processes with GDH immunoreactivity in the globus pallidus (GP) were as dense as those in the neostriatum, and were clumped within the neuropil between the large fiber bundles that coursed through the structure (Fig. 6, *D, E*).

Other telencephalic nuclei. The basolateral amygdaloid complex (BL, BLV, BM, LA; Fig. 6*E*) exhibited intense GDH immunoreactivity in evenly distributed, irregularly shaped cells and processes. In contrast, the corticomedial group (Me, ACo, PMCo; Fig. 6, *E, F*) was sparsely labeled. One exception was the central nucleus (Ce; Fig. 6*E*) of the corticomedial group, which exhibited more processes containing GDH immunoreactivity.

The septohippocampal nucleus (SHi; Fig. 6*B*) contained an extremely dense plexus of twiglike processes with GDH immunoreactivity. These processes were uniformly oriented in parallel to the fiber tracts running mediolaterally through the nucleus. With the exception of external portions of the nucleus of the diagonal band (DB), which also contained dense, twiglike processes with GDH immunoreactivity along the brain surface (Fig. 6*C*) and dense labeling in the horizontal limb (HDB; Fig. 6*D*), more delicate, branched processes of moderate distributions were seen in the related septal nuclei.

Thalamus. In the thalamus, numerous shaggy, branched processes and cell bodies immunolabeled for GDH had features of protoplasmic astrocytes. The most intensely labeled nuclei in the dorsal thalamus were the rhomboid (Rh), the central medial (CM), and the paracentral (PC) nuclei of the intralaminar group (Fig. 6*E*). In the ventral thalamus, the reticular nucleus (Rt) and zona incerta (ZI) contained the densest collections of labeled cells (Fig. 6*E*). The pattern of labeling in the neuropil of the

←

of sections prepared as in *B*, except for a higher concentration of glutaraldehyde. The GDH-labeling in the cytoplasm of neurons is far more evident in the cortex (*D*) than in the CP (*B, F*). Neuronal labeling is indicated by *arrows* in *B, D*, and *F*. *f*, Myelinated fibers. Bar: *A, B, G, H*, 50 μm; *C–F*, 25 μm.

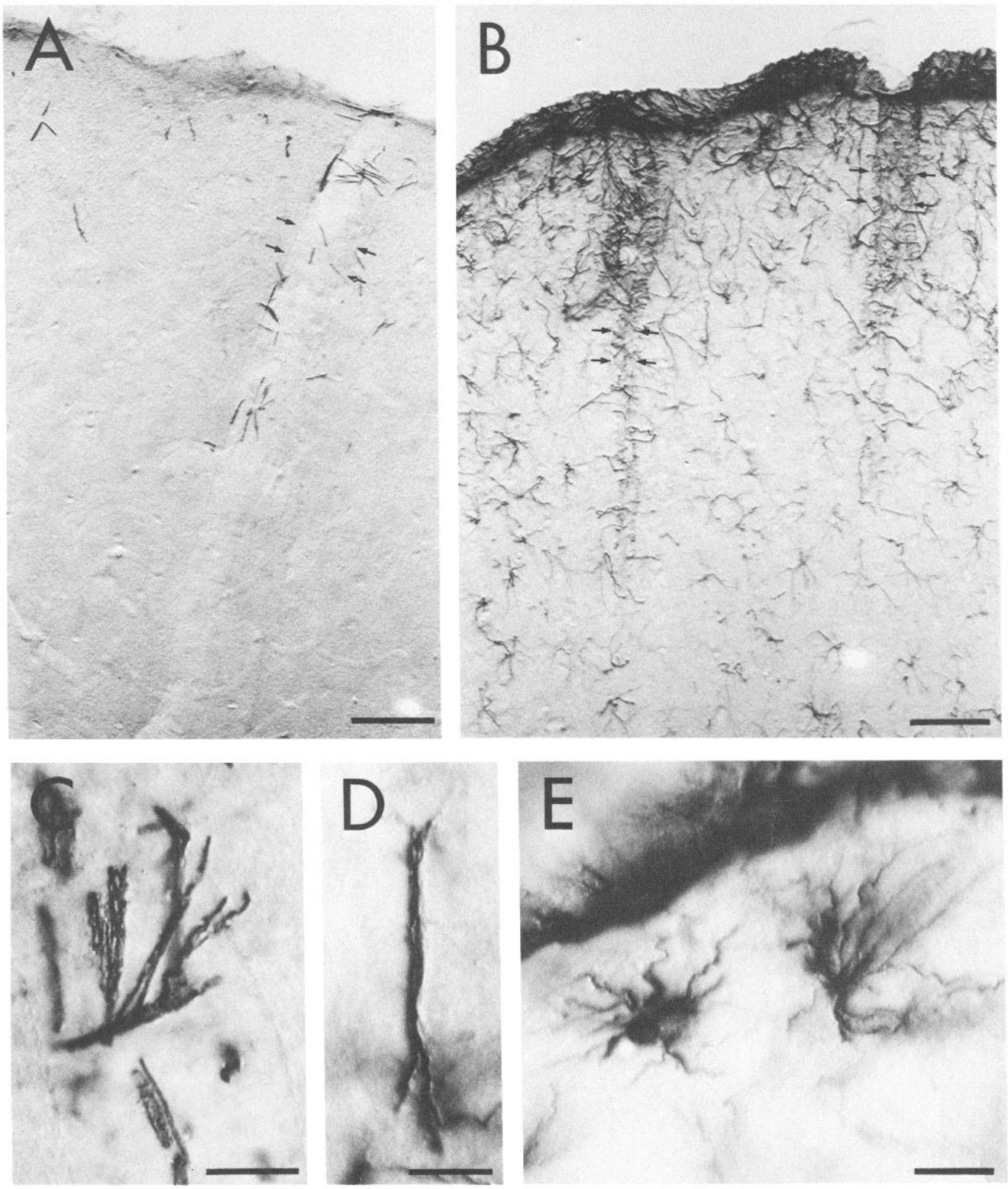

Figure 2. Localization of GDH and GFAP in the anterior cingulate cortex. *A,* Low-magnification micrograph showing the "twiglike" processes with GDH immunoreactivity near the cortical surface and in relation to the walls (*arrows*) of a penetrating blood vessel. *B,* Low-magnification micrograph showing a corresponding area from the same brain processed in parallel for the localization of GFAP. Numerous labeled cells are seen throughout the cortical layers but are especially dense near the walls (*arrows*) of blood vessels. *C, D,* Higher-magnification micrographs of the fibrillar twig-type processes labeled with GDH and GFAP, respectively. *E,* Higher-magnification micrograph showing the labeling of GFAP in the more widely distributed, presumably protoplasmic, astrocytes, which generally lacked detectable GDH immunoreactivity in the cerebral cortex. Bars: *A, B,* 50 μm; *C–E,* 10 μm.

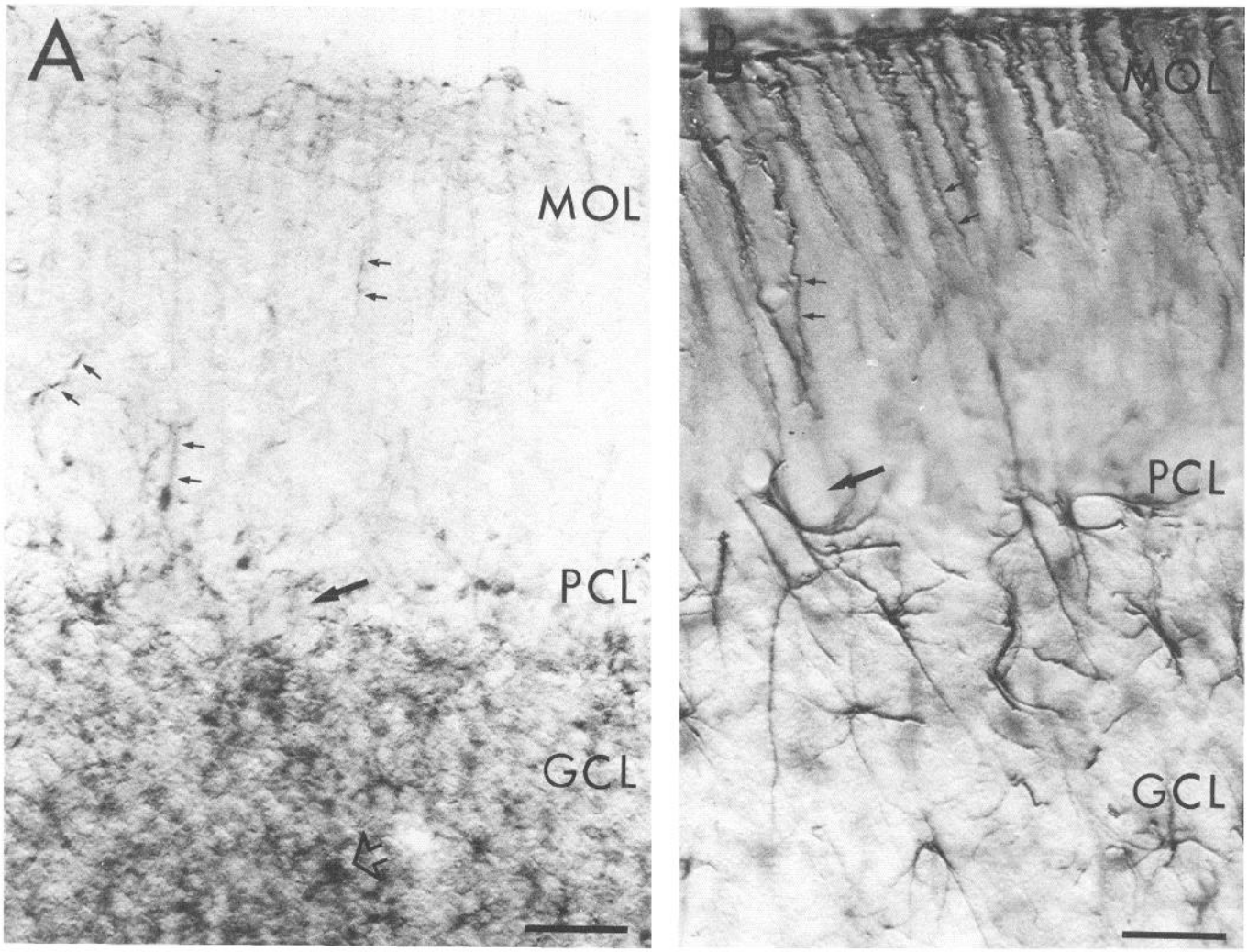

Figure 3. Localization of GDH and GFAP in the cerebellar cortex. *A,* Micrograph showing the fine veil-like processes labeled with GDH (*double arrows*) that radiate through the molecular layer (*MOL*) of the cerebellum. These processes encircle Purkinje cells (*PCL*) (*larger arrow*). More dense GDH labeling of presumed glial cells and processes is indicated with a *large open arrow* in the granule cell layer (*GCL*). *B,* Micrograph showing the localization of GFAP in glial processes (*double arrows*) of the same cerebellar layers seen in *A*.

ventral thalamus was broken up by the many fiber bundles of the thalamic radiation and fields of Forel. The subthalamic nucleus (Sb; Fig. 6*E*) also contained an extensive plexus of labeled processes. The remaining thalamic nuclei contained moderate, low, or no detectable immunoreactivity for GDH.

Hypothalamus. In the hypothalamus, the highest density of processes with GDH immunoreactivity was seen in the suprachiasmatic (Sch) and supraoptic (SO) nuclei (Fig. 6*D*). The labeled processes in these nuclei appeared more stippled or varicose than in other regions. More characteristic glia-like processes labeled with GDH were densely distributed in the dorsal hypothalamic area (DA; Fig. 6*E*), and were somewhat less numerous in the rostral part of the medial and the lateral preoptic nuclei (MP and LPO; Fig. 6*D*). As shown in Figure 6*E*, labeled processes were rarely detected in the remaining hypothalamic nuclei.

Fiber tracts. Some of the most intensely immunoreactive cells and processes were seen within fiber tracts in the forebrain; other tracts remained clearly unlabeled. The processes were numerous in the corpus callosum and external capsule (cc, gcc, ec; Fig. 6, *A–G*; Fig. 1*C*), internal capsule (ic; Fig. 6*E*), anterior commissure (aca, ac, acp; Fig. 6, *A–C*), lateral olfactory tract (lo; Fig. 6, *A–D*), dorsal fornix (Fig. 6*E*), fimbria (fx, fi; Fig. 6, *D, E*), optic tract (opt, oc, sox; Fig. 6, *D, E*), and cerebral peduncle (cp; Fig. 6, *F, G*). The fornix (f, fx; Fig. 6, *D, E*), the stria medullaris (sm; Fig. 6*D*), and the mammillothalamic tract were less densely labeled, while the rostral continuation of the superior cerebellar peduncle, the mammillotegmental tract, and the stria terminalis (st; Fig. 6, *D, E*) had almost no detectable labeling. Finally, immunoreactivity for GDH was seen in processes within the medial lemniscus (ml; Fig. 6, *F–H*) only in regions near pontine nuclei.

Midbrain

In the midbrain, only the central gray, substantia nigra, pontine nuclei, and a few nuclei in the reticular formation, along with selective fiber tracts, had noteworthy densities of processes or cells with GDH immunoreactivity.

In the central gray, immunoreactive processes were seen throughout the region, but the dorsal and caudal areas were more heavily labeled (CG, CGD; Fig. 6, *F, G*). The labeled cells and processes in the substantia nigra (SNC, SNR; Fig. 6*F*) were

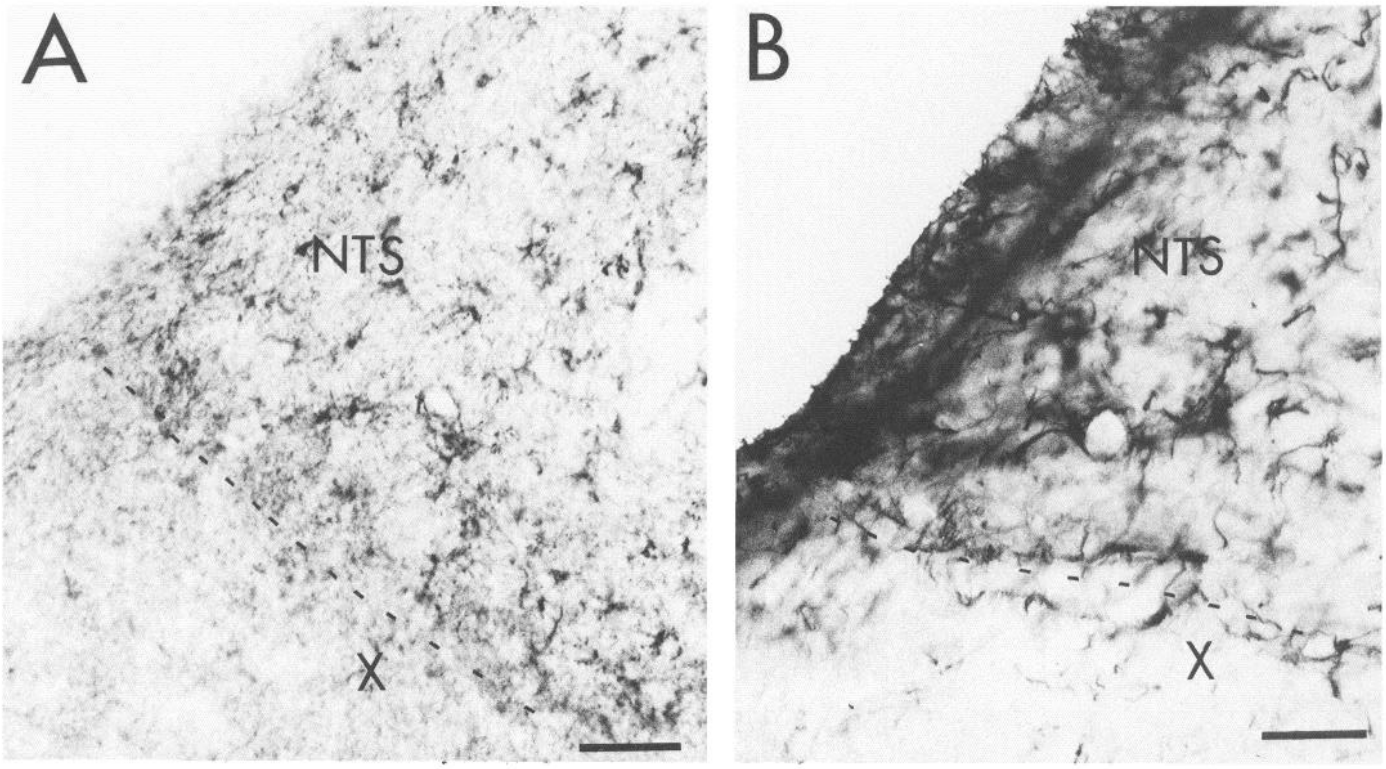

Figure 4. Localization of GDH and GFAP in the nucleus of the solitary tract. *A, B,* Micrographs showing the respective localizations of GDH and GFAP in glia of the rostral nucleus of the solitary tract (*NTS*) and adjacent motor nucleus of the vagus (*X*). With both antisera, the intensity of labeling of the astrocyte-like processes is much darker in the NTS than in the X. *Dotted line* demarks the boundary between NTS and X. Bar: 40 μm.

almost exclusively restricted to the areas adjacent to the cerebral peduncles (cp), which were themselves heavily labeled (Fig. 6*F*).

The pontine nuclei (Pn), the afferent corticopontine fibers within the longitudinal fibers of the pons (lfp), and the efferent transverse fibers of the pons (tfp) all exhibited prominent labeling of cells and processes (Fig. 6*G*). Some of the processes were like those in other heavily myelinated structures, such as the globus pallidus, and others were of the straight, twiglike morphology.

Among nuclear groups of the reticular formation, the cuneiform (Cnf; Fig. 6*G*) and lateral dorsal tegmental (LDTg; Fig. 6*G*) nuclei exhibited densely labeled cells with radiating and sometimes varicose processes, while the dorsal and ventral parabrachial nuclei contained more modest densities of labeled cells.

Fiber tracts containing the highest density of immunoreactive cells and processes included the cerebral peduncle (cp; Fig. 6*F*) and superior cerebellar peduncle (scp; Fig. 6*G*). Two auditory pathways, i.e., the lateral lemniscus (ll; Fig. 6*G*) and the brachium of the inferior colliculus (bic; Fig. 6*G*), contained a more moderate density of labeling.

Hindbrain

Reticular nuclei that project to the cerebellum, namely, the paramedian (PMn; Fig. 6*J*) and lateral reticular (LRt; Fig. 6, *I, J*) nuclei of the medulla, as well as the reticulotegmental nucleus of the pons (RtTg; Fig. 6*G*) (reviewed in Carpenter, 1978) contained high densities of cells and processes with immunoreactivity for GDH. The pyramidal tracts (py; Fig. 6, *H–J*) and trapezoid body (tz; Fig. 6*H*) continued to exhibit intensely immunoreactive processes through the level of decussation. The area of the tract of the central tegmentum and locus coeruleus were labeled moderately. Of the raphe complex, only the dorsal nuclei and the dorsal part of the median nuclei (DR and MR; Fig. 6*G*) exhibited detectable levels of immunoreactivity in astrocyte-like cells or processes.

Intense labeling of glial processes in cranial nerves was restricted to the selective subnuclei and tracts associated with the trigeminal (spV, SpVO, SpVI, mV; Fig. 6, *G, H*), facial (VII; Fig. 6*H*), acoustic (VIIIn; Fig. 6*H*), and vagus (X; Fig. 6, *I, J*), including the nucleus ambiguus (Amb; Fig. 6, *I, J*).

→

Figure 5. Dual peroxidase and autoradiographic labeling for GDH and GFAP antisera. Micrographs show the labeling for GDH (brown PAP reaction) with superimposed silver grains (^{125}I-autoradiography), revealing the localization of GFAP in the neocortex (*A, B*), caudate putamen (*D*), and perirhinal fissure area (*F*). Micrographs in *C, E,* and *G* show sections corresponding to *A, B, D,* and *F* that were similarly dually labeled, but with the omission of GDH antiserum. *Open arrows* in *A–C* point to pial surfaces, the *single small arrow* in *A* to the dually immunoreactive twiglike processes, the *double arrows* in *A, B, D,* and *F* to the astrocyte of the more conventional morphology, and the *arrowheads* to the GDH-immunoreactive but GFAP-nonimmunoreactive processes. The *bold arrows* in *C, E* and *G* point to the GFAP-immunoreactive processes. Note that these are devoid of cross-reactive rabbit PAP products. Bar: *A–C,* 50 μm; *D–G,* 25 μm.

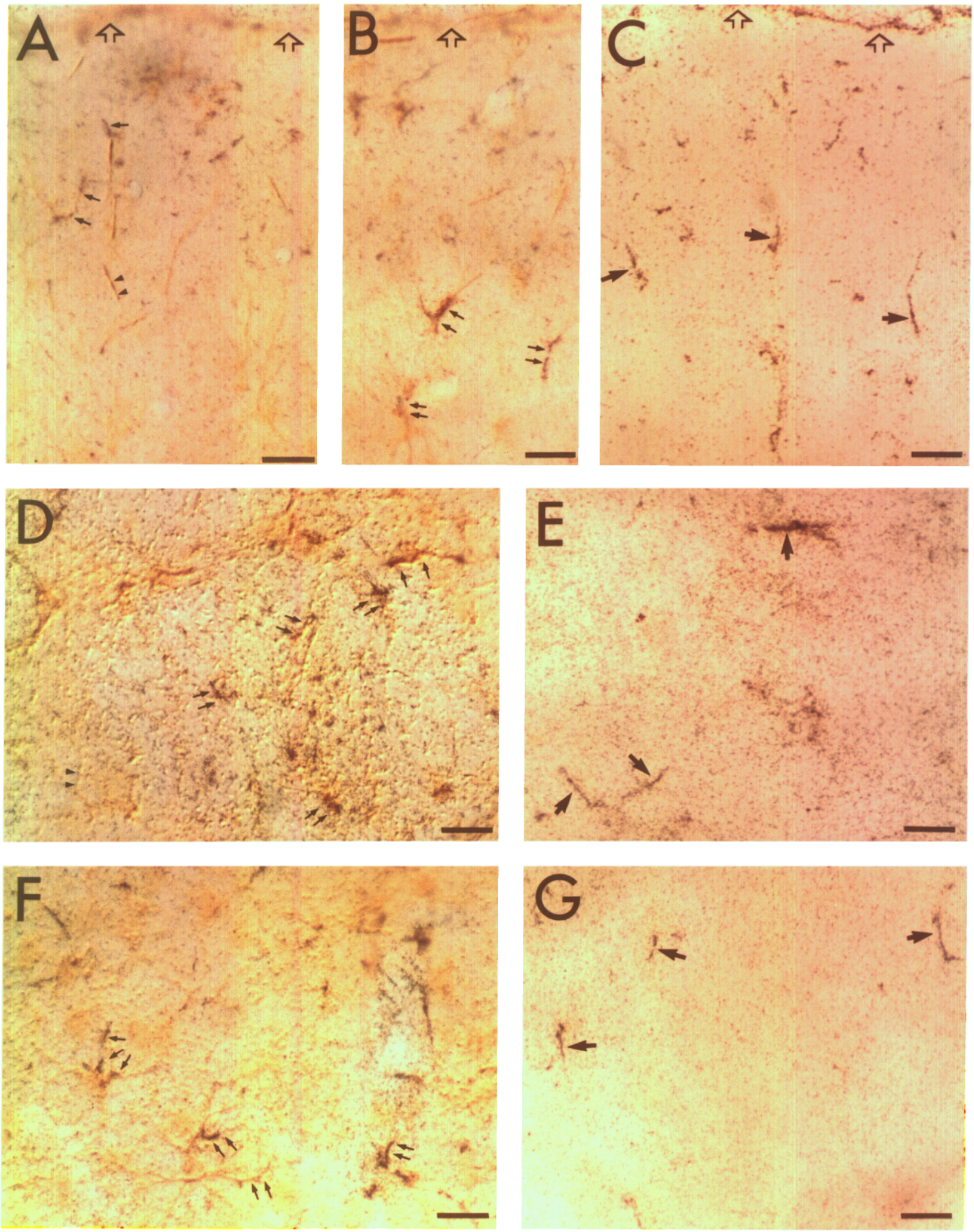
A
B
C
D
E
F
G

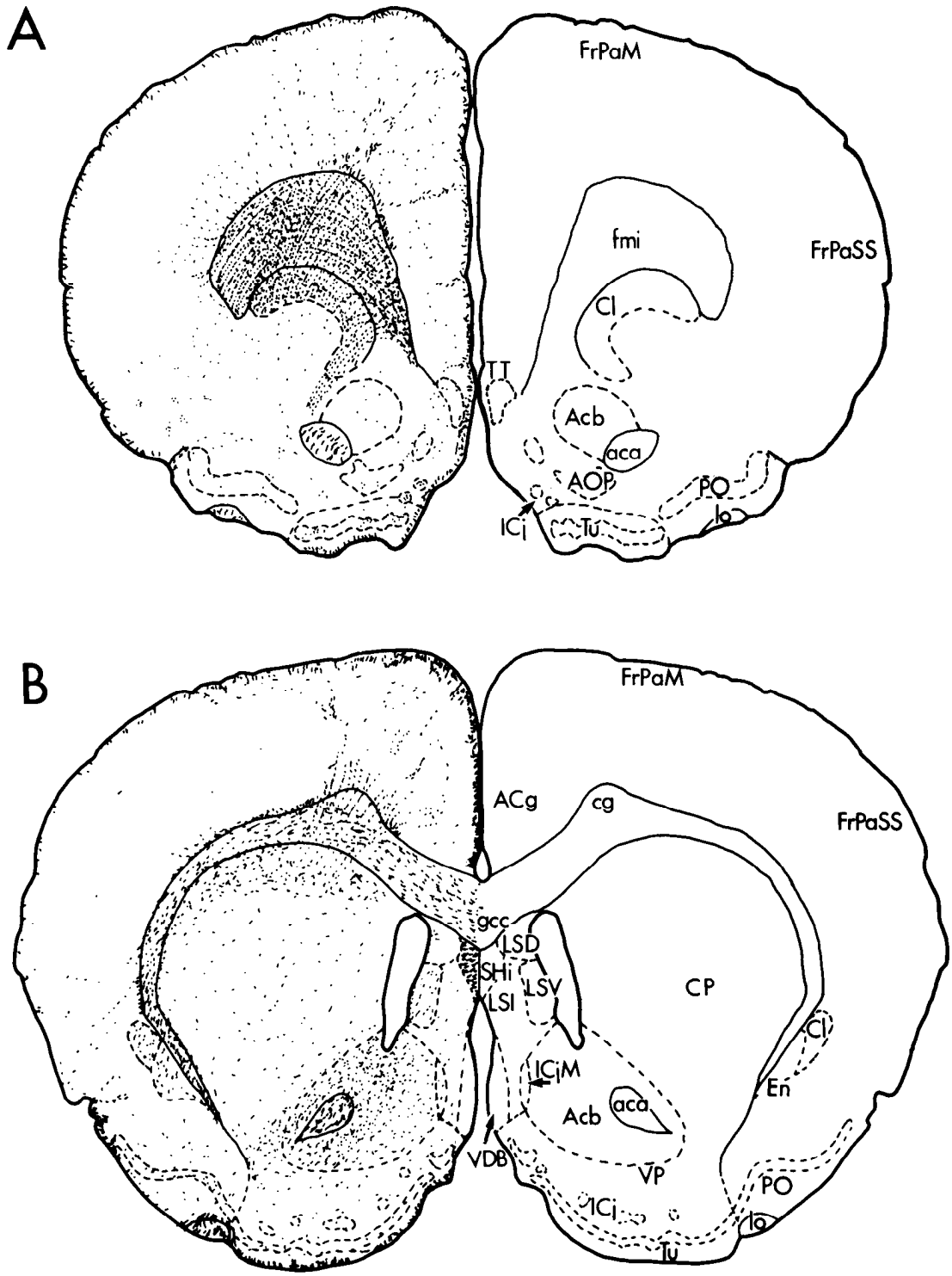

Figure 6. Distribution of GDH-immunoreactive processes. Schematic drawings of the left halves of coronal sections, *A–J,* represent GDH-immunoreactive processes, drawn with the aid of a camera lucida. Nuclei boundaries are delineated with *dashed lines* and identified on *right halves* of the drawings with *upper-case letters,* while fiber tract boundaries are delineated with *continuous lines* and identified with *lower-case letters.* Further details are as described in Materials and Methods. Bar: *A–H,* 2.28 mm; *I, J,* 1.14 mm (see Appendix for abbreviations).

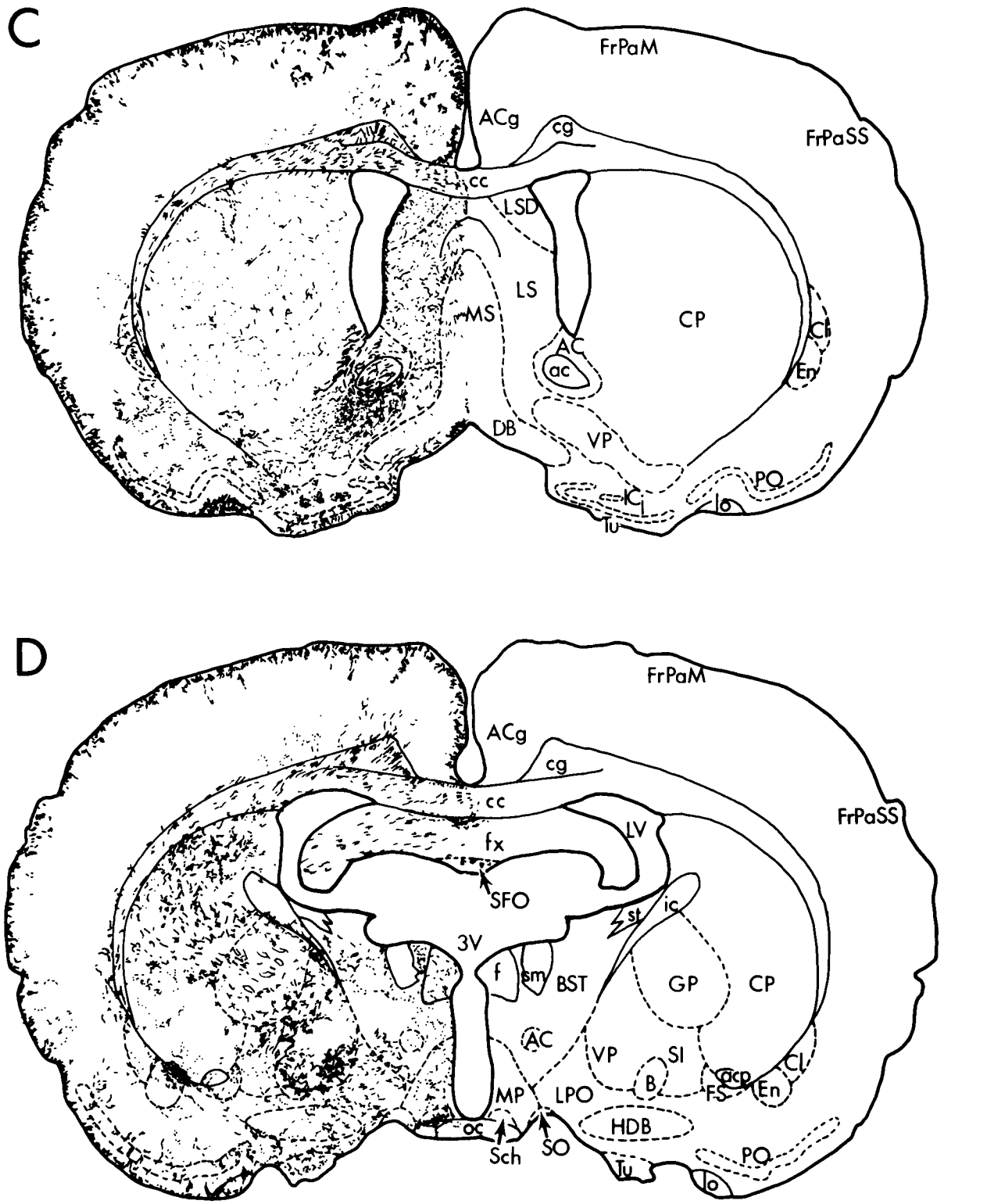

Figure 6. Continued.

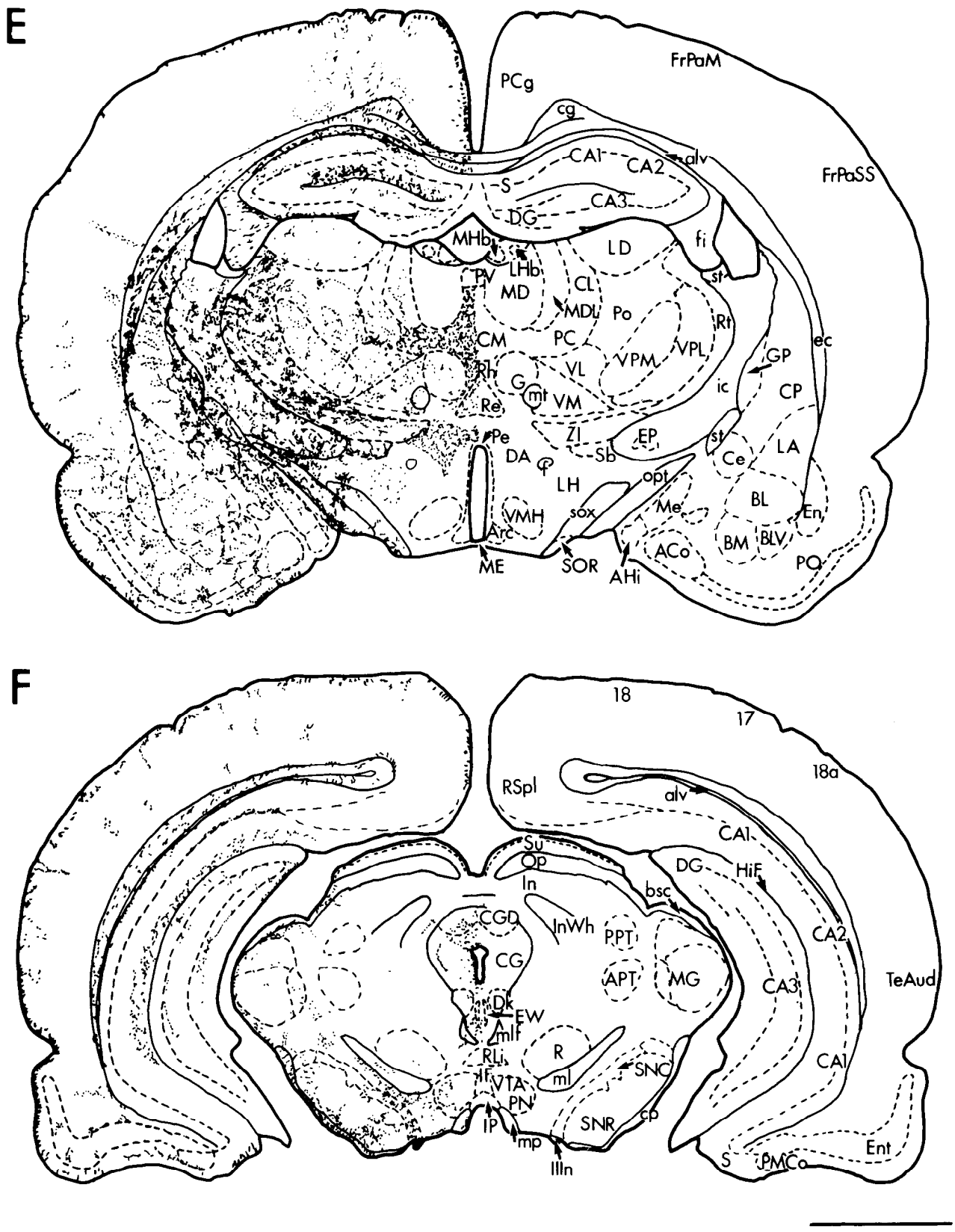

Figure 6. Continued.

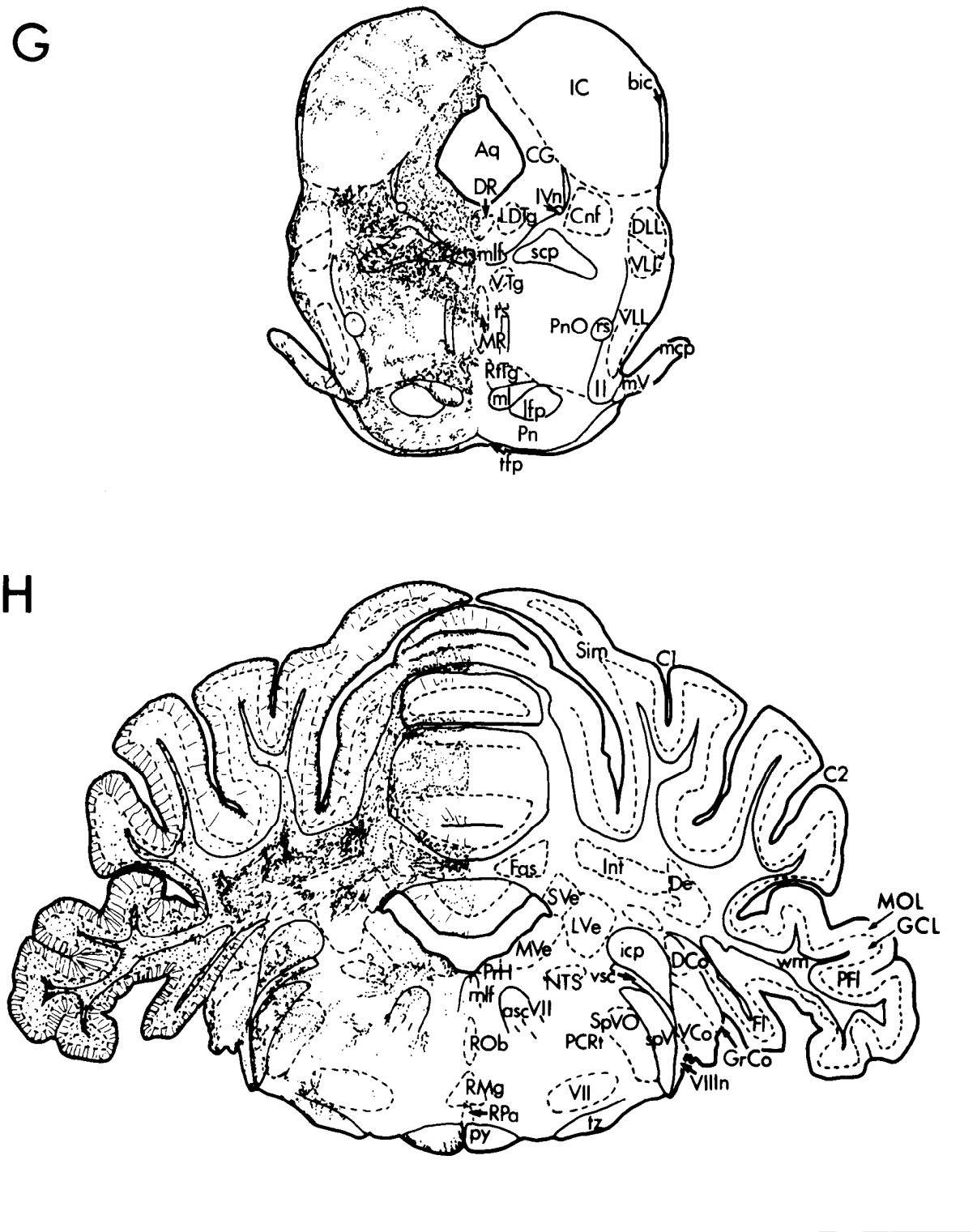

Figure 6. Continued.

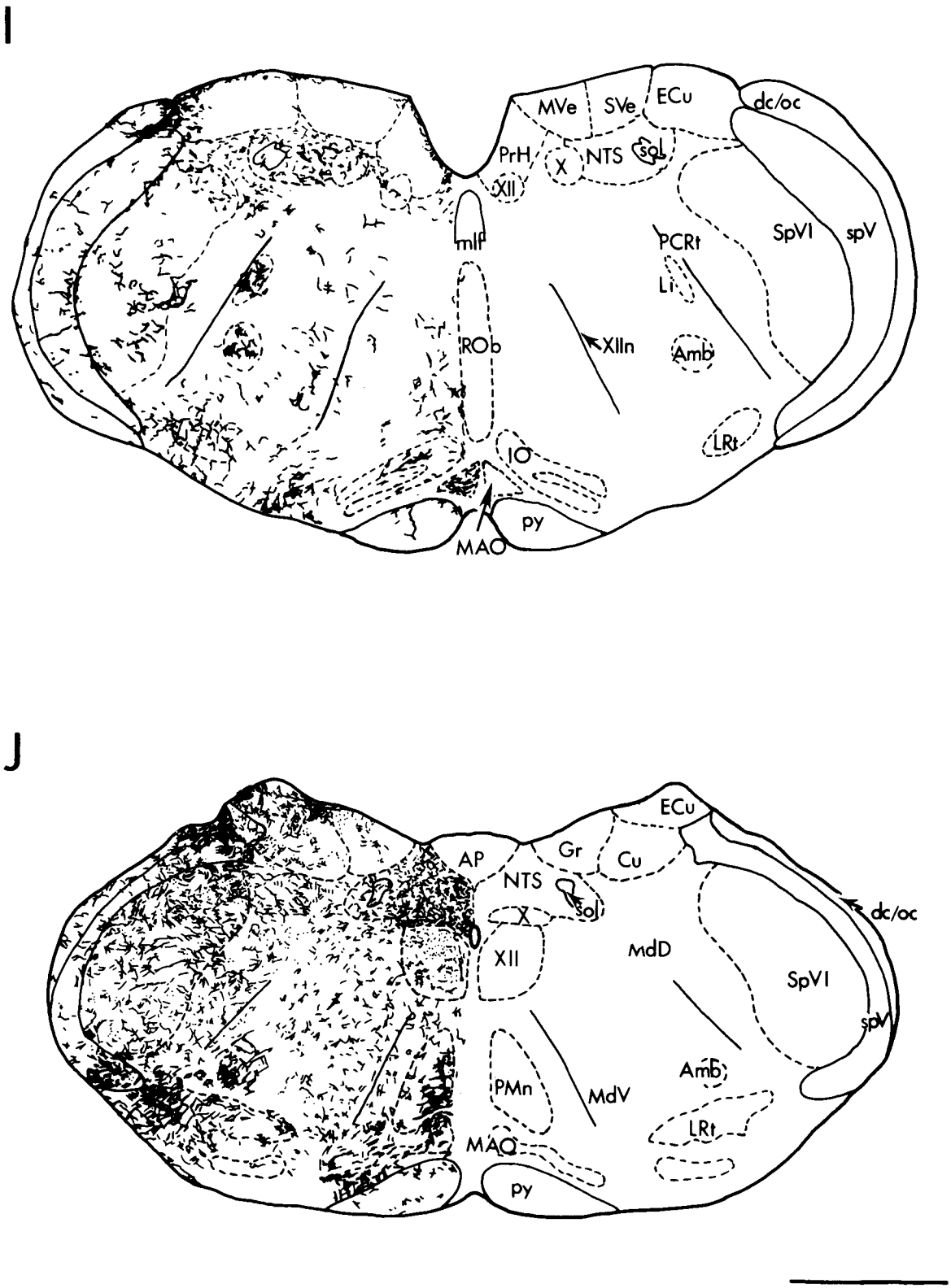

Figure 6. Continued.

Of the nuclei and fiber tracts of the dorsal column, the nucleus of the external cuneate (ECu; Fig. 6, *I, J*) contained the highest density of labeled processes within the brain. The cuneate nucleus (Cu; Fig. 6*J*) and its fiber tract, and the gracilis nucleus (Gr; Fig. 6*J*) and its fiber tract were also densely labeled.

The inferior olive complex (IO) was another structure where intensely GDH-immunoreactive processes were numerous. These processes were fasciculated and closely wrapped around fiber bundles (Fig. 6*I*). Of the inferior olive complex, the medial accessory olive (MAO; Fig. 6, *I, J*) exhibited particularly intense labeling for GDH in small branched processes.

Cerebellum

The cells and processes with GDH immunoreactivity were fairly evenly distributed throughout the rostrocaudal extent of the various folia of the cerebellar cortex (Fig. 6*H*). The entire granule cell layer (GCL) exhibited a patchy, diffuse labeling. Processes with moderate intensity of GDH immunoreactivity were evident in the molecular layer. Many labeled processes resembled the fine varicose branches of Bergmann glia (called the "velate astrocytes" by Palay and Chan-Palay, 1974). Labeling for GDH was also seen in other types of glial processes (Ramón y Cajal, 1911) that appeared to radiate from various depths within the entire thickness of the molecular layer and were particularly evident in the floculonodular lobules.

The deep cerebellar nuclei, i.e., the fastigial (Fas), the interpositus (Int), and the dentate (De) (Fig. 6*H*), contained equal and moderate densities of processes with GDH immunoreactivity. Many labeled processes coursed parallel to the bundles of axons in the white matter near the deep cerebellar nuclei. Other myelinated bundles of fibers in the cerebellum also contained numerous delicate, GDH-immunoreactive processes oriented parallel to their longitudinal axes.

Discussion

Characterization of the antigenic GDH

The present detection of intense labeling of GDH in glia in aldehyde-fixed sections of rat brain, using an antiserum raised against bovine liver GDH, supports earlier evidence for a high degree of conservation of the molecular structure of the enzyme among various species (Smith et al., 1975) and organs (Chee et al., 1979). However, the detection of immunoreactivity was highly dependent on the procedures used for tissue preparation. The optimal labeling seen in paraformaldehyde-fixed Vibratome sections using 0.2% Triton X-100 probably reflects the conditions necessary for the antisera to reach certain intramolecular antigenic sites or subcellular compartments with minimal diffusion of GDH. Lai et al. (1986) have shown that GDH in rat brain is present in mitochondrial and nuclear fractions. GDH in isolated mitochondria can be solubilized in 0.1% Triton X-100, while nuclear GDH is soluble only in elevated concentrations of Triton X-100 (0.3%) and salt (150 mM KCl). Colon et al. (1986) also found that rat brain contained at least 2 kinds of GDH, differing in their susceptibilities to detergent extraction. Our results are consistent with the possible existence of multiple forms of the enzyme. It seems likely that the nuclear fraction that was difficult to solubilize even in unfixed tissues was never made freely accessible to the antisera under the experimental conditions that yielded optimal cytoplasmic labeling of glia in the present study. However, because of intense labeling in the cytoplasm, nuclear labeling of glia may have been obscured. Alternatively, the antiserum used in the present study may also have recognized a form of GDH distinct from the nuclear form characterized by Lai et al. (1986). Under the conditions of our study, the antisera may recognize primarily a Triton-insoluble GDH that is more GTP-, NADH/NADPH-, and heat-sensitive than is the soluble form, and which has been proposed to be "non-mitochondrial" (Colon et al., 1986).

Glial versus neuronal localization of GDH

The results of this study have shown that, in Triton-treated sections, GDH is primarily localized to cells having the morphological characteristics of astrocytes (Kosaka and Hama, 1986). In certain processes, dual labeling with GDH and GFAP further supports the concept that many GDH-containing cells are astrocytes. However, certain processes showed only GFAP, while others were immunolabeled exclusively for GDH. This would not be unexpected, since immunoreactivity for GFAP is principally localized to large shafts of processes containing glial filaments (Kosaka and Hama, 1986), and GDH would more likely be distributed in fine ramifications of processes enveloping synapses. Methodological factors such as differences in penetration of antisera or more superficial detection of autoradiographic labeling probably also contribute to the differential detection of GDH and GFAP. In addition, GDH may be found in a relatively small population of astrocytes containing GFAP, and may also be detected in oligodendrocytes or microglia. There is evidence strongly suggesting that oligodendrocytes (GFAP-negative, galactocerebroside-positive) and astrocytes (GFAP-positive, galactocerebroside-negative) arise from a common progenitor cell (Raff et al., 1983) and retain common antigenic determinants even after maturation (Brenner et al., 1986). Also, the matter of whether or not microglia arise from astrocytes or from blood monocytes remains unsettled (Miles and Chou, 1986; Schelper and Adrian, 1986). In light of these reports, it would be of interest to determine the ontogeny of expression of the antigenic form of glial GDH in relation to the other marker proteins by means of immunocytochemical double-labeling.

While the most intense reaction for GDH was seen in glial processes in the present study, neuronal soma with varying intensities of immunoreactivity also were detected whenever Triton X-100 was omitted from the labeling procedure. The low-intensity cytoplasmic labeling seen in virtually all neurons is probably attributable to levels of the enzyme associated with the metabolic pools of glutamate. More intense neuronal labeling for GDH in certain regions, such as the cerebral cortex, could be associated with the neurotransmitter L-glutamate, as described for glia in the next section.

The difficulty in detecting neuronal labeling for GDH in the presence of Triton X-100 is probably attributable to the masking of faint immunoreactivity in neurons by more intense labeling of glia or, alternatively, to the greater solubility of neuronal GDH or its association with lipids that are extracted by detergents.

Distribution of GDH in relation to glutamatergic pathways

Detailed rostrocaudal mapping of GDH-immunoreactive glial cells and processes in the present study revealed a distribution remarkably similar to known glutamatergic pathways. In the neocortex, we detected the highest densities of twiglike processes containing GDH immunoreactivity within layer I, particularly in the anterior pole, and also accompanying large, orthogonally

oriented blood vessels through layer III. Corresponding with this pattern is the uptake of ^{3}H-D-aspartate within cortical slices, which has been shown to be highest in layer I (Fonnum et al., 1981). These observations are further supported by Monaghan and Cotman's (1985) characterization of *N*-methyl-D-aspartate-sensitive glutamate receptors and the characterization by Halpain et al. of ^{3}H-glutamate receptors, which indicate the presence of a laminar distribution that is highest within superficial layers, more anteriorly than caudally. In the cerebellum, the laminar distribution of these receptors also closely matches the GDH distribution, and in the inferior colliculus, *N*-methyl-D-aspartate-sensitive glutamate receptor binding exhibits a dorsal-to-ventral downward gradient (Monaghan and Cotman, 1985), much like the distribution of GDH-immunoreactive processes seen within this area. On the basis of the present results, the demonstrated glutamate receptor binding may include both glia and neurons within receptive regions.

The above and other studies have demonstrated convincingly that the neostriatum, the accumbens nucleus, and, to a lesser extent, the substantia nigra receive glutamatergic fibers from the frontal cortex, while the lateral septal nucleus receives glutamatergic fibers from the hippocampal formation, and the amygdala from the frontal, pyriform, and entorhinal cortices (reviewed in Fonnum, 1984). In the present study, all of these areas demonstrated moderate to intense GDH immunoreactivity.

The high densities of glial processes with GDH immunoreactivity were detected in the intralaminar (rhomboid, central medial, and paracentral) and ventral (reticular nucleus and zona incerta) thalamic nuclei. The question of whether these areas are sites of termination or of origin remains unsettled (Streit, 1980; Rustioni and Cuenod, 1982). In support of the theory that certain thalamic nuclei are termination sites for pathways containing L-glutamate are reports of high densities of *N*-methyl-D-aspartate-sensitive receptors in these ventral and midline nuclei (Monaghan and Cotman, 1985).

Hindbrain areas that receive cortical afferents (reviewed in Carpenter, 1978), namely, (1) the reticular nuclei (reticulotegmental, lateral reticular, and paramedian nuclei), (2) the sensory relay nuclei (gracile, cuneate, external cuneate, sensory trigeminal, and solitary tract nuclei), (3) the inferior olive, and (4) the pontine nuclei, exhibited dense populations of GDH-immunoreactive processes. In accordance with this, many corticofugal systems (reviewed in Streit, 1984) and cerebellar projecting pathways (reviewed in Ottersen and Storm-Mathisen, 1984) are believed to be glutamatergic. Our finding of large numbers of glial cells with GDH immunoreactivity in the intermediate and caudal portions of the medial nuclei of the solitary tracts is also consistent with electrophysiological evidence that suggests that L-glutamate is one of the neurotransmitters of afferent nerve fibers from arterial baroreceptors (Talman et al., 1980).

The brain stem reticular and sensory relay nuclei are reported to contain only moderate densities of glutamate receptors (Halpain et al., 1984; Monaghan and Cotman, 1985), which suggests that GDH immunoreactivity may reflect factors other than the degree of glutamatergic innervation. It is interesting that these areas do exhibit intense levels of another mitochondrial enzyme, cytochrome oxidase (Claude, 1946; Wong-Riley, 1976), indicative of high levels of tonic synaptic activity (Wong-Riley et al., 1978, Wong-Riley 1979; Aoki et al., 1987). Conceivably, the neuronal activity may determine the rate of turnover of glutamate released from axon terminals.

The present localization of GDH in glia of presumed glutamatergic pathways supports recent studies on neuron–glia interactions (reviewed in Hertz et al., 1983) in maintaining the compartmentalization of metabolic and neurotransmitter pools of L-glutamate. Besides their well-documented role in the control of interstitial ion composition and volume (reviewed in Abbott, 1986), astrocytes take up glutamate with a capacity that is higher than that of neurons (Huck et al., 1984). Astrocytes, then, can convert the glutamate to α-ketoglutarate and return the product to the tricarboxylic acid cycle of neurons (Dennis and Clark, 1977). Alternatively, the astrocytes may use glutamine synthetase to convert glutamate to glutamine for its return to the amino acid pool of astrocytes and neurons (Bradford et al., 1978). The active uptake and metabolism of glutamate by astrocytes are consistent with the present detection of GDH in regions where L-glutamate is actively released by axon terminals.

Involvement of GDH in glutamate cytotoxicity

Glutamate and its analogs, kainic and ibotenic acid are well-known excitotoxins when present in excess amounts within glutamate-receptive areas (Van Harreveld and Fifková, 1971), including the temporal lobe (Olney, 1985) and striatum (McGeer and McGeer, 1976; Coyle et al., 1977). L-Glutamate also has been implicated in neurodegenerative changes following metabolic insults, such as hypoglycemia (Wieloch, 1985) and ischemia (Rothman, 1984; Simon et al., 1984), since these damages can be prevented by prior, central applications of antagonists to glutamate receptors.

As noted above, the hindbrain areas with the highest concentrations of GDH were structures that project to the cerebellum. These areas, together with the GDH-rich granule cell layer of the cerebellar cortex, characteristically undergo atrophy in extrapyramidal motor disorders of the olivopontocerebellar type (Yamaguchi et al., 1982; Duvoisin et al., 1983; Plaitakis et al., 1984). As postulated by Plaitakis et al. (1984), the high levels of GDH may be necessary for protection against glutamate cytotoxicity in areas having active glutamatergic neurotransmission. Thus, these areas would be expected to be the first to show neuronal degeneration following a systemic deficiency of GDH. GDH-deficient patients exhibit "multiple-system degeneration," suggestive of alterations of the caudate putamen and globus pallidus, the hippocampus and other limbic structures, the cortex, the oculomotor nerve, lateral vestibular nucleus, cerebellum, brain stem, frontal lobes, hypothalamic and thalamic areas. The present detection of high densities of GDH immunoreactivity in glial processes in all of these areas strongly supports the concept that degenerative changes in specific regions of the CNS may be associated with deficiencies of GDH. However, the reports of GDH deficiency in patients with multiple systems degeneration were based on measurements of GDH activity in leukocytes and fibroblasts. It would be of interest to confirm that the GDH activity within the CNS and, in particular, within the brain stem, pontine, and cerebellar areas is similarly deficient in these patients.

Appendix.—Abbreviations used in Figure 6

AC, ant. commissural n.
ac, ant. commissure
aca, ant. commissure, ant.
Acb, accumbens n.
ACg, ant. cingulate cortex
ACo, ant. cortical n. of amygdala

acp, ant. commissure, post.
AHi, amygdalohippocampal a.
alv, alveus of hippocampus
Amb, ambiguus n.
AOP, ant. olfactory n., post.
AP, a. postrema
APT, ant. pretectal n.
Aq, aqueduct
Arc, arcuate n. of hypothalamus
ascVII, ascending fibers of facial nerve
B, cells of basal n. of Meynert
bic, brachium of inferior colliculus
BL, basolateral n. of amygdala
BLV, basolateral n. of amygdala, vent.
BM, basomedial n. of amygdala
bsc, brachium of sup. colliculus
BST, bed n. of stria terminalis
C1, crus 1 of ansiform lobule
C2, crus 2 of ansiform lobule
CA1, field CA1 of Ammon's horn of hippocampus
CA2, field CA2 of Ammon's horn of hippocampus
CA3, field CA3 of Ammon's horn of hippocampus
cc, corpus callosum
Ce, central n. of amygdala
CG, central gray
cg, cingulum
CGD, central gray, dorsal
CL, central lat. n. of thalamus
Cl, claustrum
CM, central med. n. of thalamus
Cnf, cuneiform n.
CP, caudate putamen
cp, cerebral peduncle, basal
Cu, cuneate n.
DA, dorsal a. of hypothalamus
DB, n. of diagonal band
DCo, dorsal cochlear n.
dc/oc, dorsal spinocerebellar tract/olivocerebellar tract
De, dentate n. of cerebellum
DG, dentate gyrus of hippocampus
Dk, n. of Darkschewitsch
DLL, dorsal n. of lat. lemniscus
DR, dorsal raphe
Dsc, lamina dissecans of entorhinal cortex
ec, ext. capsule
ECu, ext. cuneate n.
En, endopyriform n.
Ent, entorhinal cortex
EP, endopeduncular n.
EW, Edinger-Westphal n.
f, postcommissural fornix
Fas, fastigial n. of cerebellum
fi, fimbria of hippocampus
Fl, flocculus
FrPaM, frontoparietal cortex, motor a.
FrPaSS, frontoparietal cortex, somatosensory a.
FS, fundus striati
fx, fornix
G, gelatinosus n. of thalamus
gcc, genu corpus callosum
GCL, granule cell layer of cerebellar cortex
GP, globus pallidus
Gr, gracile n.
GrCo, granule cell layer of cochlear n.
HDB, n. of horizontal limb of diagonal band
HiF, hippocampal fissure
IC, inf. colliculus
ic, int. capsule
ICj, islands of Calleja
ICjM, islands of Calleja, major island
icp, inf. cerebellar peduncle
IF, interfascicular n.
IIIn, oculomotor nerve
In, intermediate gray layer of sup. colliculus
Int, interpositus n. of cerebellum
InWh, intermediate white layer of superior colliculus
IO, inf. olive
IP, interpeduncular nucleus, cent.
IVn, trochlear nerve
LA, lat. n. of amygdala
LD, lat. dorsal n. of thalamus
LDTg, laterodorsal tegmental n.
lfp, longitudinal fasciculus of pons
LH, lat. hypothalamic a.
LHb, lat. habenula of epithalamus
Li, linear n. of medulla
ll, lat. lemniscus
lo, lat. olfactory tract
LPO, lat. preoptic a.
LRt, lat. reticular n.
LS, lat. septal n.
LSD, lat. septal n., dorsal
LSI, lat. septal n., intermediate
LSV, lat. septal n., vent.
LV, lat. ventricle
LVe, lat. vestibular n.
MAO, med. accessory olive
mcp, middle cerebellar peduncle
MD, mediodorsal n. of thalamus
MDL, mediodorsal n. of thalamus, lat.
MdD, reticular n. of medulla, dorsal
MdV, reticular n. of medulla, vent.
ME, median eminence
Me, med. n. of amygdala
MG, med. geniculate n. of thalamus
MHb, med. habenula of epithalamus
ml, med. lemniscus
mlf, med. longitudinal fasciculus
MOL, molecular layer of cerebellar cortex
MP, med. preoptic a.
mp, mammillary peduncle
MR, median raphe n.
MS, med. septal n.
mt, mammillothalamic tract
mV, motor root of trigeminal nerve
MVe, med. vestibular n.
NTS, n. of solitary tract
oc, optic chiasm
Op, optic nerve layer of sup. colliculus
opt, optic tract
PaS, parasubiculum
PBg, parabigeminal n.
PC, paracentral n. of thalamus
PCg, posterior cingulate cortex

PCRt, parvocellular reticular n.
Pe, periventricular n. of hypothalamus
PFl, paraflocculus
PMCo, posteromedial cortical n. of amygdala
PMn, paramedian reticular n.
PN, paranigral n.
Pn, pontine n.
PnO, pontine reticular n., oral
PO, primary olfactory cortex
Po, post. complex of thalamus
PPT, post. pretectal n.
PrH, prepositus hypoglossal n.
PrS, presubiculum
PV, paraventricular n. of epithalamus
py, pyramidal tract
R, red n.
Re, reuniens n. of thalamus
Rh, rhomboid n. of thalamus
RLi, rostral linear n. of raphe
RPa, raphe pallidus n.
RMg, raphe magnus n.
ROb, raphe obscurus
RR, retrorubral n.
rs, rubrospinal tract
RSpl, retrosplenial cortex
Rt, reticular n. of thalamus
RtTg, reticulotegmental n. of pons
S, subiculum
Sb, subthalamic a.
Sch, suprachiasmatic n. of hypothalamus
scp, sup. cerebellar peduncle
SFO, subfornical organ
SHi, septohippocampal n.
SI, substantia innominata
Sim, simple lobule
sm, stria medullaris of thalamus
SNC, substantia nigra, pars compacta
SNR, substantia nigra, pars reticulata
SO, supraoptic n. of hypothalamus
sol, solitary tract
sox, supraoptic decussation
spV, spinal tract trigeminal nerve
SpVI, n. of spinal trigeminal nerve, interpositus
SpVO, n. of spinal trigeminal nerve, oral
st, stria terminalis
Su, superficial gray layer of sup. colliculus
SVe, sup. vestibular n.
Te, temporal cortex
TeAud, temporal cortex, auditory a.
tfp, transverse fibers of pons
ts, tectospinal tract
TT, taenia tecta
Tu, olfactory tubercle
tz, trapezoid body
VCo, ventral cochlear n.
VDB, n. of the vertical limb of diagonal band
VII, facial n.
VIIIn, vestibulocochlear nerve
VL, vent. lat. n. of thalamus
VLL, vent. n. of lat. lemniscus
VM, vent. med. n. of thalamus
VMH, ventromedial a. of hypothalamus
VP, vent. pallidum
VPL, vent. post. n. of thalamus, post.
VPM, vent. post. n. of thalamus, med.
vsc, vent. spinocerebellar tract
VTA, vent. tegmental a.
VTg, vent. tegmental n.
wm, white matter of cerebellar cortex
X, dorsal motor n. of vagus
XII, hypoglossal n.
XIIn, hypoglossal nerve
ZI, zona incerta of thalamus
3V, third ventricle
17, a. 17 (striate) of cortex
18, a. 18 (peristriate) of cortex
18a, a. 18a (peristriate) of cortex.

References

Abbott, N. J. (1986) The neuronal microenvironment. Trends Neurosci. *9:* 3–8.

Aoki, C., T. A. Milner, K.-F. R. Sheu, J. P. Blass and V. M. Pickel (1987) Glial glutamate dehydrogenase: ultrastructural localization and regional distribution in relation to the mitochondrial enzyme, cytochrome oxidase. J. Neurosci. Res. (in press).

Bignami, A., L. F. Eng, D. Dahl, and C. T. Uyeda (1972) Localization of the glial fibrillary acidic protein in astrocytes by immunofluorescence. Brain Res. *43:* 429–435.

Bradford, H. F., H. K. Ward, and A. J. Thomas (1978) Glutamine—a substrate for nerve endings. J. Neurochem. *30:* 1454–1459.

Brenner, T., R. P. Lisak, A. Rostami, D. E. Pleasure, and D. H. Silberberg (1986) Astrocytes, oligodendrocytes, and Schwann cells share a common antigenic determinant that cross-reacts with myelin basic protein: Identification with monoclonal antibody. J. Neurosci. *6:* 1925–1933.

Carpenter, M. B. (1978) *Core Text of Neuroanatomy,* 2nd Ed., Williams and Wilkins, Baltimore, MD.

Chee, P. Y., J. L. Dahl, and L. A. Fahien (1979) The purification and properties of rat brain glutamate dehydrogenase. J. Neurochem. *33:* 53–60.

Claude, A. (1946) Fractionation of mammalian liver cells by differential centrifugation: II. Experimental procedures and results. J. Exp. Med. *84:* 61–89.

Colon, A. D., A. Plaitakis, A. Perakis, S. Berl, and D. D. Clarke (1986) Purification and characterization of a soluble and particulate glutamate dehydrogenase from rat brain. J. Neurochem. *46:* 1811–1819.

Cotman, C. W., A. C. Foster, and T. Lanthorn (1981) An overview of glutamate as a neurotransmitter. Adv. Biochem. Psychopharmacol. *27:* 1–27.

Coyle, J. T., R. Schwarcz, J. P. Bennett, and P. Campochiaro (1977) Clinical, neuropathologic and pharmacologic aspects of Huntington's disease: Correlates with a new animal model. Prog. Neuropsychopharmacol. *1:* 13–30.

Dennis, S. C., and J. B. Clark (1977) The pathway of glutamate metabolism in rat brain mitochondria. Biochem. J. *168:* 521–527.

Duvoisin, R. C., S. Chokroverty, F. Lepore, and W. Nicklas (1983) Glutamate dehydrogenase deficiency in patients with olivopontocerebellar atrophy. Neurology *33:* 1322–1326.

Fonnum, F. (1984) Glutamate: A neurotransmitter in mammalian brain. J. Neurochem. *42:* 1–11.

Fonnum, F., A. Soreide, I. Kvale, J. Walker, and I. Walaas (1981) Glutamate in cortical fibers. Adv. Biochem. Psychopharmacol. *27:* 29–42.

Graham, L. T., and M. H. Aprison (1969) Distribution of some enzymes associated with the metabolism of glutamate, aspartate, γ-aminobutyrate and glutamine in cat spinal cord. J. Neurochem. *16:* 559–566.

Halpain, S., C. M. Wieczorek, and T. C. Rainbow (1984) Localization of L-glutamate receptors in rat brain by quantitative autoradiography. J. Neurosci. *4:* 2247–2258.

Hedreen, J. C., S. J. Bacon, and D. L. Price (1985) A modified histochemical technique to visualize acetylcholinesterase-containing axons. J. Histochem. Cytochem. *33:* 134–140.

Hertz, L., E. Kvamme, E. G. McGeer, and A. Schousboe (eds.) (1983) *Glutamine, Glutamate and GABA in the Central Nervous System,* Alan R. Liss, New York.

Huck, S., F. Grass, and H. Hörtnagl (1984) The glutamate analogue α-aminoadipic acid is taken up by astrocytes before exerting its gliotoxic effect *in vitro.* J. Neurosci. *4:* 2650–2657.

Jones, E. G. (1985) *The Thalamus,* Plenum, New York.

Kosaka, T., and K. Hama (1986) Three-dimensional structure of astrocytes in the rat dentate gyrus. J. Comp. Neurol. *249:* 242–260.

Lai, J. C. K., K.-F. R. Sheu, Y. T. Kim, D. D. Clarke, and J. P. Blass (1986) The subcellular localization of glutamate dehydrogenase (GDH): Is GDH a marker for mitochondria in brain? Neurochem. Res. *11:* 733–744.

Leong, S. F., and J. B. Clark (1984) Regional development of glutamate dehydrogenase in the rat brain. J. Neurochem. *43:* 106–111.

McGeer, E. G., and P. L. McGeer (1976) Duplication of biochemical changes of Huntington's chorea by intrastriatal injection of glutamic and kainic acids. Nature *263:* 517–519.

Miles, J. M., and S. M. Chou (1986) LN-1 as a marker for microglia in paraffin sections. In Neuroimmunology Symposium Abstracts, London, Ontario, p. 12.

Monaghan, D. T., and C. W. Cotman (1985) Distribution of N-methyl-D-aspartate-sensitive L-^{3}H-glutamate-binding sites in rat brain. J. Neurosci. *5:* 2902–2919.

Nicklas, W. J. (1984) Amino acid metabolism in the central nervous system: Role of glutamate dehydrogenase. Adv. Neurol. *41:* 245–253.

Olney, J. W. (1985) Excitatory transmitters and epilepsy-related brain damage. Int. Rev. Neurobiol. *27:* 337–362.

Ottersen, O. P., and J. Storm-Mathisen (1984) Glutamate- and GABA-containing neurons in the mouse and rat brain, as demonstrated with a new immunocytochemical technique. J. Comp. Neurol. *229:* 374–392.

Palay, S. L., and V. Chan-Palay (1974) *Cerebellar Cortex. Cytology and Organization,* Springer-Verlag, Berlin.

Paxinos, G., and C. Watson (1982) *The Rat Brain in Stereotaxic Coordinates,* Academic, New York.

Peters, A., and E. G. Jones (1984) *Cerebral Cortex,* Vols. 1–4, Plenum, New York.

Pickel, V. M. (1981) Immunocytochemical methods. In *Neuroanatomical Tract-Tracing Methods,* L. Heimer and M. J. Robards, eds., pp. 483–509, Plenum, New York.

Pickel, V. M., J. Chan, and T. A. Milner (1986) Autoradiographic detection of ^{125}I-secondary antiserum: A sensitive light and electron microscopic labeling method compatible with peroxidase immunocytochemistry for dual localization of neuronal antigens. J. Histochem. Cytochem. *34:* 707–718.

Plaitakis, A., S. Berl, and M. D. Yahr (1984) Neurological disorders associated with deficiency of glutamate dehydrogenase. Ann. Neurol. *15:* 144–153.

Raff, M. C., R. H. Miller, and M. Noble (1983) A glial progenitor cell that develops *in vitro* into an astrocyte or an oligodendrocyte depending on the culture medium. Nature *303:* 390–396.

Ramón y Cajal, S. (1928) *Histologie du Système Nerveux de l'Homme et des Vertèbres, 1909–1911,* Oxford U. P., London.

Rothman, S. (1984) Synaptic release of excitatory amino acid neurotransmitter mediates anoxic neuronal death. J. Neurosci. *4:* 1884–1891.

Rustioni, A., and M. Cuénod (1982) Selective retrograde transport of D-aspartate in spinal interneurons and cortical neurons of rats. Brain Res. *236:* 143–155.

Ryder, E. (1980) Enzymatic profile of mitochondria isolated from selected brain regions of young adult and one-year-old rats. J. Neurochem. *34:* 1550–1552.

Schelper, R. L., and E. K. Adrian (1986) Monocytes become macrophages; they do not become microglia: A light and electron microscopic autoradiographic study using ^{125}iododeoxyuridine. J. Neuropathol. Exp. Neurol. *45:* 1–19.

Simon, R. P., J. H. Swan, T. Griffiths, and B. S. Meldrum (1984) Blockade of *N*-methyl-D-aspartate receptors may protect against ischemic damage in the brain. Science *226:* 850–852.

Smith, E. L., B. M. Austen, K. M. Blumenthal, and J. F. Nya (1975) Glutamate dehydrogenases. Enzymes *11A:* 293–367.

Sternberger, L. A. (1979) *Immunocytochemistry,* Wiley, New York.

Streit, P. (1980) Selective retrograde labeling indicating the transmitter of neuronal pathways. J. Comp. Neurol. *191:* 429–463.

Streit, P. (1984) Glutamate and aspartate as transmitter candidates for systems of the cerebral cortex. In *Cerebral Cortex,* E. G. Jones and A. Peters, eds., pp. 119–144, Plenum, New York.

Talman, W. T., M. H. Perrone, and D. J. Reis (1980) Evidence for L-glutamate as the neurotransmitter of baroreceptor afferent nerve fibers. Science *209:* 813–815.

Van Harreveld, A., and E. Fifková (1971) Light and electron microscopic changes in central nervous tissue after electrophoretic injection of glutamate. Exp. Mol. Pathol. *15:* 61–81.

Watkins, J. C., and R. H. Evans (1981) Excitatory amino acid transmitters. Annu. Rev. Pharmacol. Toxicol. *21:* 165–204.

Wenthold, R. J. (1980) Glutaminase and aspartate aminotransferase decrease in the cochlear nucleus after lesion of the auditory nerve. Brain Res. *190:* 293–297.

Wieloch, T. (1985) Hypoglycemia-induced damage prevented by an *N*-methyl-D-aspartate antagonist. Science *230:* 681–683.

Wong-Riley, M. T. T. (1976) Endogenous peroxidatic activity in brain stem neurons as demonstrated by their staining with diaminobenzidine in normal squirrel monkey. Brain Res. *108:* 257–277.

Wong-Riley, M. (1979) Changes in the visual system of monocularly sutured or enucleated cats demonstrable with cytochrome oxidase histochemistry. Brain Res. *171:* 11–28.

Wong-Riley, M. T. T., M. M. Merzenich, and P. A. Leake (1978) Changes in endogenous enzymatic reactivity to DAB induced by neuronal inactivity. Brain Res. *141:* 185–192.

Yamaguchi, T., K. Hayashi, H. Murakami, K. Ota, and S. Maruyama (1982) Glutamate dehydrogenase deficiency in spinocerebellar degenerations. Neurochem. Res. *7:* 627–636.